Bull. Chem. Soc. Ethiop. **2023**, 37(4), 1047-1054.
DOI: https://dx.doi.org/10.4314/bcse.v37i4.19

ISSN 1011-3924
Printed in Ethiopia
Online ISSN 1726-801X

REGRESSION MODELLING FOR CONCENTRATION DEPENDENT MASS DENSITY AND SPECIFIC VOLUME OF AQUEOUS SURFACTANT SOLUTIONS

Selvaraju Sivamani*, Jeanifer Manganaan Ehilla, Saikat Banerjee and Manickam Vijayanand

Engineering Department, University of Technology and Applied Sciences, Salalah College of Technology, Salalah, Oman

(Received August 29, 2022; Revised October 18, 2022; Accepted February 21, 2023)

ABSTRACT. In the present work, mathematical models relating mass density and specific volume of solution with concentration for aqueous solutions of anionic (sodium lauryl sulfate - SLS) and cationic (cetyltrimethylammonium bromide - CTAB) surfactants (0-10% (w/w)) have been investigated. The experimental studies were performed to study the effect of solution concentration on mass density and specific volume of solution. Mass density increases, and specific volume decreases with an increase in solution concentration for both surfactants. Linear, quadratic, cubic, quartic, quintic, and exponential models were fitted to the experimental data to check the applicability. The models were validated based on the coefficient of determination (R^2) and the sum of square of error (SSE) to be unity and zero, respectively. Modelling results reveal that the quintic model was fitted to study the effect of density on solution concentration for both surfactants.

KEY WORDS: Density, Surfactant, Cetyltrimethylammonium bromide, Sodium lauryl sulfate, Modelling, Regression

INTRODUCTION

Surfactants (or surface-active agents) are one of the most versatile materials in chemical process industries. They are used in various industries, from household detergents to drilling muds, food, and pharmaceuticals [1]. The surfactant is called non-ionic if the head group has no charge. It is called anionic or cationic, depending on whether the head group has a negative or positive charge. The surfactant is zwitterionic if it includes both positive and negative groups. The most used surfactants utilized in the industry are anionic and cationic. Alkyl sulfates and quaternary ammonium salts are examples of anionic and cationic surfactants, respectively [2].

Since surfactants are amphiphilic, they absorb at the air-water. They position themselves at the interface such that the hydrophobic part is in the air and the hydrophilic part is in the water. As a result, interfacial tension reduces [3]. The surface tension of water is high due to the strong cohesive forces between water molecules. The addition of surfactants would decrease surface tension because the intermolecular forces between the surfactant and the water molecule are much smaller than those between two water molecules. Micelles form when the surfactant concentration is high [4].

Fluid concentration-dependent density is a significant parameter in various areas of research and development as well as in the commercial market such as healthcare and safety, protection of consumer and environment, etc. [5]. Another significant application of concentration-dependent density is quality controlling soft drink, petrochemical, alcoholic beverages (beer, spirits, wine), fuels (including biodiesel and bioethanol), personal care products, pharmaceuticals, etc. [6]. Concentration-dependent density is used to specify and describe a pure substance and determines the density of the binary mixture. Therefore, it gives information about the composition of the mixture [7].

*Corresponding author. E-mail: sivmansel@gmail.com

Mathematical modelling is a set of equations (models) that explains the behaviour of a system. In other words, models are the mathematical representation of physical models or data [8]. Models are of two types - theoretical and empirical models. Theoretical models explain the basic mechanism of the process, whereas empirical models are used for forecasting [9]. The process of modelling requires both domain and mathematical knowledge (Figure 1). Domain knowledge is used to identify problem statements, select significant predictor and response variables, and generate experimental data relating to independent and dependent variables. Mathematical knowledge is required to select univariate and multivariate models involving single or multiple coefficients [10].

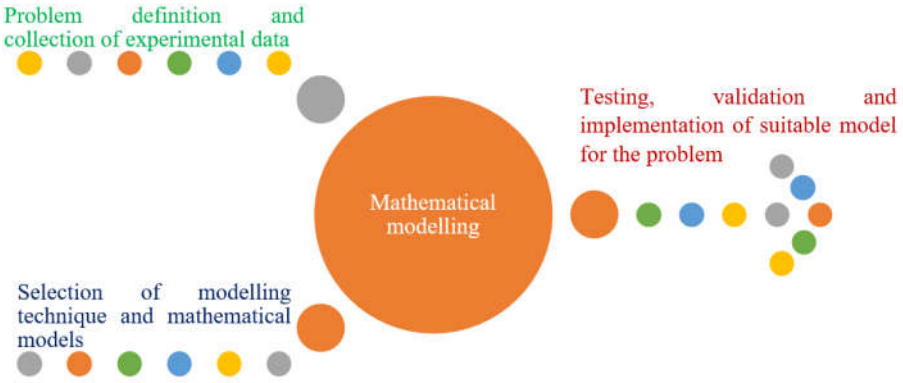

Figure 1. Modelling process.

Moreira *et al.* modelled kinematic viscosity with solution concentration and temperature simultaneously, based on previous models for respective binary systems [11]. Khounvilay and Sittikijyothin characterized tamarind seed gum as a seed polysaccharide from *Tamarindus indica* L. for physicochemical and rheological properties [12]. Simion *et al.* developed mathematical correlations between density and viscosity with parameters such as temperature and concentration [13]. Grigoraş *et al.* established mathematical models relating density and dynamic viscosity with factors such as temperature and concentration since it is established that the physicochemical properties present a significant influence on appropriate transport pipes dimensions and industrial equipment choosing/designing processes [14].

Thakur *et al.* investigated the influence of concentration (0.125-1% w/v) on viscosity and surface tension of tamarind gum [15]. Reynolds *et al.* compared the viscosity of $NaNO_2$ and $NaNO_3$ aqueous solutions to provide an opportunity to determine the relative importance of anion size versus the strength of anion interaction with water [16]. Arshad *et al.* compared the density and viscosity of ternary solutions with the few available data from the literature and showed a good agreement between experimental and model-predicted values [17]. Banerjee *et al.* studied the rheological behaviour of partially hydrolysed polyacrylamide polymer and sodium dodecyl sulphate (SDS) surfactant solutions through viscosity measurement and mathematical regression modelling [18]. Karunarathne *et al.* performed artificial neural network modelling (ANN) for CO_2 loaded aqueous amine mixtures. The results from the ANN models are in good agreement with measured properties with less than 1% average absolute relative deviation (AARD) [19].

The literature reported developed correlation/mathematical modelling between physiochemical/rheological properties of solutions, and the successfulness of modelling was identified through statistical parameters. As the limited literature is available on modelling for physicochemical properties of aqueous surfactant solutions, the present work focusses on

developing mathematical models to relate mass density and specific volume with the concentration of solution for SLS and CTAB surfactants.

EXPERIMENTAL

Materials

Surfactants were purchased from Sigma Aldrich - Merck, Bengaluru, India. Double distilled water was used in the experiments unless specified. Aqueous surfactant solutions were prepared by dissolving the required amount of surfactant in a specified volume of water. Pycnometer, available in the Chemical Engineering laboratory of University of Technology and Applied Sciences, Salalah College of Technology, was utilized to measure the mass density of solutions in the experiments.

Experimental methods

Washed and dried beakers (6 numbers) were taken. Solutions prepared by adding surfactants and water were taken at different concentrations (0, 1, 2, 3, 4, and 5 g in 50 mL of water in each beaker with concentrations equivalent to 0, 20, 40, 60, 80 and 100 g/L). The mass density of solutions at different concentrations were calculated using pycnometer by noting the mass of empty pycnometer, mass of pycnometer with solution, and pycnometer volume. All the experiments were performed in triplicate and the mean value was taken as response. A reciprocal of mass density, specific volume, was calculated from mass density [20]. Mass density was calculated using the following Equation (1):

$$Mass\ density\ of\ solution\ \rho_s = \frac{(W_2 - W_1)}{V} \quad (1)$$

where, W_1 and W_2 are mass of empty pycnometer and pycnometer with solution, respectively, V is volume of pycnometer, respectively.

Mathematical modelling

The common univariate empirical models involving multiple coefficients are linear, polynomial (quadratic, cubic, quartic, and quintic), and non-polynomial (exponential, logarithmic and power) as shown in Table 1. Linear, quadratic, cubic, quartic, and quintic models are first-, second-, third, fourth- and fifth-order forms of polynomial equations. Polynomial models can be used without any limitations [21]. However, exponential, logarithmic and power models are non-linear. So, their linear forms, used to evaluate the coefficients, are also provided in Table 1. Non-linear equations are used with limitations. For example, logarithmic and power models cannot be used for negative and zero values in either independent or dependent variables. Likewise, exponential models cannot be used when corresponding independent and dependent variables are zero. So, linear, quadratic, cubic, quartic, quintic, and exponential models were selected in the present study [22].

Table 1. Univariate empirical models involving multiple coefficients.

S. No.	Category	Type of model	Non-linear form	Linear form
1.	Linear	Linear	$Y = A+B.X$	-
2.	Polynomial	Quadratic	$Y = A+B.X+C.X^2$	-
3.		Cubic	$Y = A+B.X+C.X^2+D.X^3$	-
4.	Non-linear	Exponential	$Y = A.e^{B.X}$	$\ln Y = \ln A + B.X$
5.		Logarithmic	$Y = A + \ln X^B$	$Y = A + B.(\ln x)$
6.		Power	$Y = A.X^B$	$\ln Y = \ln A + B.(\ln x)$

Mathematical modelling was performed in Microsoft Excel 2019. Model testing was performed by fitting the experimental data to the univariate models, and the goodness of fit of the model was evaluated by the coefficient of determination (R^2) and the sum of square of error (SSE). In statistics, $R^2$and SSE are the measures of fitness of empirical models to the experimental or observed data [23]. $R^2$and SSE are calculated by using the following Equation (2) and (3), respectively:

$$R^2 = 1 - \frac{SSE}{SST} \tag{2}$$

$$SSE = (Y_e - Y_p)^2 \tag{3}$$

where SSE and SST are sum of squares of error and total sum of squares, Y_e and Y_p are experimental and predicted dependent variable, respectively. In general, R^2 value varies from 0 to 1. Sometimes, models exhibit negative values for R^2, which indicate that the data are not in agreement with the models. R^2 value of zero means that none of the variation in dependent variables corresponds to independent variables. The value of 1 means that variation in dependent variables corresponds to independent variables. For example, the value between 0 and 1 of 0.92 means that 92% variation of dependent variables corresponds to independent variables [24].

The tested model was validated by performing experiments within the range of independent variables to obtain dependent variables because the model is applicable only for the range of predictor variables. If the experimental value fits well with the predicted value, the model is validated [25]. From the model validation, suitable univariate models are selected based on R^2 = 1 and SSE = 0 and proceeded for implementation, noting that the final models are validated for the problem.

RESULTS AND DISCUSSION

Effect of concentration of aqueous surfactant solutions on mass density and specific volume

Figure 2(a) illustrates the effect of the concentration of aqueous CTAB solution on mass density and specific volume. When the concentration increased from 0 to 100 g/L, the mass density of solution is equal to mass density of solvent, i.e. water at initial concentration. As the concentration increased gradually from 20 g/L, mass density increases, and specific volume decreases due to the addition of solute to solvent. Specific volume is an inverse parameter of mass density. Hence, it exhibits reverse variation to mass density [26]. However, the variation between mass density and specific volume at different concentrations were negligible because of the small amount of solute added.

Figure 2(b) illustrates the effect of the concentration of aqueous SLS solution on mass density and specific volume. The mass density increases, and specific volume decreases with an increase in concentration from 0 to 100 g/L. The variation between mass density of CTAB solution was lesser than SLS, and the variation between specific volume of CTAB solution was greater than SLS, which may be due to its molecular weight. The molar mass of CTAB is greater than SLS [27, 28].

The experimental data was fitted to the below models as given in the Equations (3)-(8),

Linear: $\rho_s = \rho_w + kC$ (3)

Quadratic: $\rho_s = \rho_w + k_1C + k_2C^2$ (4)

Cubic: $\rho_s = \rho_w + k_1'C + k_2'C^2 + k_3'C^3$ (5)

Quartic: $\rho_s = \rho_w + k_1''C + k_2''C^2 + k_3''C^3 + k_4''C^4$ (6)

Quintic: $\rho_s = \rho_w + k_1'''C + k_2'''C^2 + k_3'''C^3 + k_4'''C^4 + k_5'''C^5$ (7)

Exponential: $\rho_s = \rho_w e^{k'X}$ (8)

where C is concentration of solution (% (w/w)) and the terms involving k are constants. An appropriate model is selected based on $R^2 = 1$ and SSE = 0.

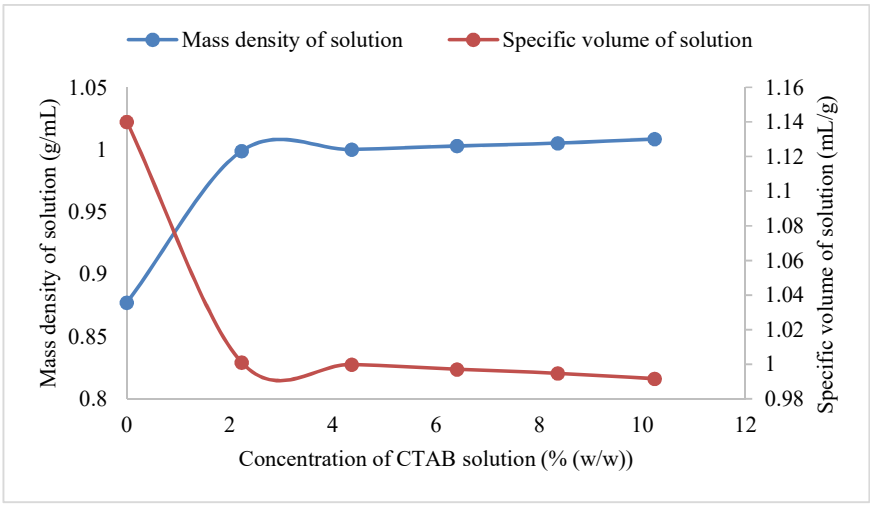

(a)

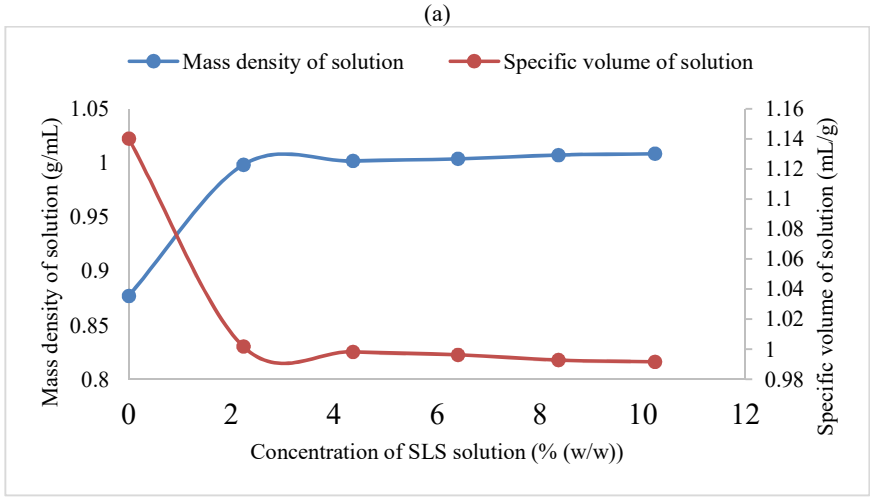

(b)

Figure 2. Effect of concentration of aqueous (a) CTAB and (b) SLS solutions on mass density and specific volume.

The fitted models for mass density and specific volume of aqueous CTAB solution were shown in Table 2(a). Mass density at zeroth concentration were 0.931, 0.896, 0.8808, 0.8774, 0.8771 and 0.9292 g/mL, respectively, for linear, quadratic, cubic, quartic, quintic, and exponential models. The experimental mass density of water was 0.8771 g/mL. The experimental value of mass density of water was equal to that obtained from the quintic model. Similarly, from

Table 2(a), specific volume at zeroth concentration were 1.0783, 1.1186, 1.1359, 1.1397, 1.1401, and 1.0762 mL/g, respectively, for linear, quadratic, cubic, quartic, quintic, and exponential models. The experimental specific volume of water was 1.1401 mL/g. The experimental value of specific volume of water was equal to that obtained from the quintic model.

Table 2. Tested models for density data of aqueous (a) CTAB and (b) SLS solutions.

(a)

Model	Mass density	R^2	Specific volume	R^2
Linear	$y = 0.0097x+0.931$	0.5193	$y = -0.0109x + 1.0783$	0.5111
Quadratic	$y = -0.0025x^2+0.0354x+0.896$	0.8287	$y = 0.0029x^2-0.0404x+1.1186$	0.8268
Cubic	$y = 0.0006x^3-0.012x^2+0.0709x+0.8808$	0.9661	$y = -0.0007x^3+0.0137x^2-0.081x+1.1359$	0.9658
Quartic	$y = -0.0001x^4+0.0032x^3-0.0287x^2+0.1029x+0.8774$	0.9968	$y = 0.0001x^4-0.0037x^3+0.0328x^2-0.1175x+1.1397$	0.9969
Quintic	$y = 0.00002x^5-0.0008x^4+0.009x^3-0.0498x^2+0.1289x+0.8771$	1	$y = -0.00003x^5+0.0009x^4-0.0102x^3+0.0567x^2-0.147x+1.1401$	1
Exponential	$y = 0.9292e^{0.0103x}$	0.5151	$y = 1.0762e^{-0.01x}$	0.5151

(b)

Model	Mass density	R^2	Specific volume	R^2
Linear	$y = 0.0098x+0.9311$	0.5247	$y = -0.011x + 1.0783$	0.5158
Quadratic	$y = -0.0025x^2+0.0359x+0.8954$	0.8407	$y = 0.0029x^2-0.0409x+1.1191$	0.8373
Cubic	$y = 0.0006x^3-0.0118x^2+0.0704x+0.8807$	0.9684	$y = -0.0007x^3+0.0135x^2-0.0805x+1.136$	0.9678
Quartic	$y = -0.0001x^4+0.0032x^3-0.0282x^2+0.102x+0.8774$	0.998	$y = 0.0001x^4-0.0037x^3+0.0323x^2-0.1166x+1.1398$	0.9979
Quintic	$y = 0.00002x^{5-}0.0006x^4+0.0077x^3-0.045x^2+0.1226x+0.8771$	1	$y = -0.00002x^5+0.0007x^{4-}0.0009x^3+0.0519x^{2-}0.1407x+1.1401$	1
Exponential	$y = 0.9292e^{0.0104x}$	0.5202	$y = 1.0768e^{-0.01x}$	0.5202

The fitted models for mass density and specific volume of aqueous SLS solution were shown in Table 2(b). Mass density at zeroth concentration were 0.9311, 0.8954, 0.8807, 0.8774, 0.8771 and 0.9292 g/mL, respectively, for linear, quadratic, cubic, quartic, quintic, and exponential models. The experimental mass density of water was 0.8771 g/mL. The experimental value of mass density of water was equal to that obtained from the quintic model. Similarly, from Table 2(b), specific volume at zeroth concentration were 1.0783, 1.1191, 1.136, 1.1398, 1.1401, and 1.0768 mL/g, respectively, for linear, quadratic, cubic, quartic, quintic, and exponential models. The experimental specific volume of water was 1.1401 mL/g. The experimental value of specific volume of water was equal to that obtained from the quintic model [29, 30]. Hence, the quintic model was found to be the suitable model for relating mass density and specific volume with concentration for aqueous solutions of anionic (sodium lauryl sulfate - SLS) and cationic (cetyltrimethylammonium bromide - CTAB) surfactants.

CONCLUSION

This work aimed to develop a mathematical model relating mass density and specific volume of solutions with the concentration of aqueous anionic and cationic surfactant solutions. The experiments were performed to study the effect of solution concentration on mass density and specific volume of solutions. Mass density increased and specific volume decreased with an increase in solution concentration for both surfactants. Linear, quadratic, cubic, quartic, quintic,

and exponential models were used to fit the experimental data. Based on R^2 and SSE, the quintic model fitted well with the experimental data. The results showed the best goodness of fit between experimental and model-predicted values.

ACKNOWLEDGMENTS

We would acknowledge our heartfelt thanks to the Management of University of Technology and Applied Sciences, Salalah College of Technology, Sultanate of Oman, for the wonderful opportunity, continuing support, and encouragement by providing necessary facilities for executing the research work.

REFERENCES

1. Abdulraheim, A.M. Green polymeric surface active agents for crude oil demulsification. *J. Mol. Liq.* **2018**, 271, 329-341.
2. Kim, T.S.; Kida, T.; Nakatsuji, Y.; Hirao, T.; Ikeda, I. Surface-active properties of novel cationic surfactants with two alkyl chains and two ammonio groups. *J. Am. Oil Chem. Soc.* **1996**, 73), 907-911.
3. Harano, K.; Nakamura, E. Interfacial chemistry of conical fullerene amphiphiles in water. *Acc. Chem. Res.* **2019**, 52, 2090-2100.
4. Lu, G.; Duan, Y.Y.; Wang, X.D. Surface tension, viscosity, and rheology of water-based nanofluids: a microscopic interpretation on the molecular level. *J. Nanoparticle Res.* **2014**, 16, 1-11.
5. Darros-Barbosa, R.; Balaban, M.O.; Teixeira, A.A. Temperature and concentration dependence of density of model liquid foods. *Int. J. Food Prop.* **2003**, 6, 195-214.
6. Marina, O.; Biernacki, M.A.; Brusic, V.; Wu, C.J. A concentration-dependent analysis method for high density protein microarrays. *J. Proteome Res.* **2008**, 7, 2059-2068.
7. Noack, K.; Kiefer, J.; Leipertz, A. Concentration-dependent hydrogen-bonding effects on the dimethyl sulfoxide vibrational structure in the presence of water, methanol, and ethanol. *ChemPhysChem*, **2010**, 11, 630-637.
8. Grundmann, H.; Hellriegel, B. Mathematical modelling: a tool for hospital infection control. *Lancet Infect. Dis.* **2006**, 6, 39-45.
9. Varini, M.; Campana, P.E.; Lindbergh, G. A semi-empirical, electrochemistry-based model for Li-ion battery performance prediction over lifetime. *J. Energy Storage* **2019**, 25, 100819.
10. Nassif, N. Single and multivariate regression models for estimating monthly energy consumption in schools in hot and humid climates. *Energy Eng.* **2013**, 110, 33-54.
11. Moreira, R.; Chenlo, F.; Saint-Olympe, A. Kinematic viscosity of aqueous solutions of ethanol and glucose in the range of temperatures from 20 to 45 ºC. *Int. J. Food Prop.* **2009**, 12, 834-843.
12. Khounvilay, K.; Sittikijyothin, W. Rheological behaviour of tamarind seed gum in aqueous solutions. *Food Hydrocolloids* **2012**, 26, 334-338.
13. Simion, A.I.; Grigoraş, C.G.; Roşu, A.M.; Gavrilă, L. Mathematical modelling of density and viscosity of nacl aqueous solutions. *Journal of Agroalimentary Processes and Technologies*, **2015**, 21, 41-52.
14. Grigoras, C.G.; Muntianu, G.; Gavrila, L. Mathematical modelling of $CaCl_2$ aqueous solutions thermophysical properties. *Sci. Study Res. Chem. Chem. Eng. Biotechnol. Food Industry* **2016**, 17, 417.
15. Thakur, S; Sharma, P.K.; Malviya, R. Influence of concentration on surface tension & viscosity of tamarind (*Tamarindus indica*) seed gum. *Annals Mol. Genet. Med.* **2017**, 1, 008-012.
16. Reynolds, J.G.; Mauss, B.M.; Daniel, R.C. The relative viscosity of $NaNO_3$ and $NaNO_2$ aqueous solutions. *J. Mol. Liq.* **2018**, 264, 110-114.

17. Arshad, M.; Easa, A.; Qiblawey, H.; Nasser, M.; Benamor, A.; Bhosale, R.; Al-Ghouti, M. Experimental measurements and modelling of viscosity and density of calcium and potassium chlorides ternary solutions. *Sci. Rep.* **2020**, 10, 1-19.
18. Banerjee, T.; Samanta, A.; Mandal, A. Mathematical regression models for rheological behavior of interaction between polymer-surfactant binary mixtures and electrolytes. *J. Dispers. Sci. Technol.* **2022**, 43, 1333-1352.
19. Karunarathne, S.S.; Chhantyal, K.; Eimer, D.A.; Øi, L.E. Artificial neural networks (ANNs) for density and viscosity predictions of CO_2 loaded alkanolamine + H_2O mixtures. *ChemEngineering* **2020**, 4, 29.
20. Sato, Y.; Nishizuka, T.; Hara, K.; Yamamura, T.; Waseda, Y. Density measurement of molten silicon by a pycnometric method. *Int. J. Thermophys.* **2000**, 21, 1463-1471.
21. Smith, J.; De Micheli, G. Polynomial methods for allocating complex components. *Proceedings of the Conference on Design, Automation and Test in Europe* **199**9; p 45.
22. Bazeia, D.; Belendryasova, E.; Gani, V.A. Scattering of kinks in a non-polynomial model. *J. Phys. Conference Series* **2017**, 934, 012032.
23. Chandrasekaran, A.P.; Sivamani, S. Statistical modeling and optimization of pretreatment for fermentable sugars production from cotton gin waste. *Energy Sources A: Recovery Util. Environ. Effects* **2018**, 40, 400-405.
24. Vijayanand, M.; Varahamoorthi, R.; Kumaradhas, P.; Sivamani, S.; Kulkarni, M.V. Regression-BPNN modelling of surfactant concentration effects in electroless NiB coating and optimization using genetic algorithm. *Surf. Coat. Technol.* **2021**, 409, 126878.
25. Maran, J.P. Statistical optimization of aqueous extraction of pectin from waste durian rinds. *Int. J. Biol. Macromol.* **2015**, 73, 92-98.
26. Petkova, B.; Tcholakova, S.; Chenkova, M.; Golemanov, K.; Denkov, N.; Thorley, D.; Stoyanov, S. Foamability of aqueous solutions: Role of surfactant type and concentration. *Adv. Colloid Interface Sci.* **2020**, 276, 102084.
27. Tiwari, S.; Mall, C.; Solanki, P.P. CMC studies of CTAB, SLS and tween 80 by spectral and conductivity methodology to explore its potential in photogalvanic cell. *Surf. Interfaces* **2020**, 18, 100427.
28. Olofintoye, O.O.; Salami, A.W. Development and assessment of a quintic polynomial model for the prediction of maximum daily rainfall in Ilorin, Nigeria. *NSE Technical Trans. Technical Publ. Nig. Soc. Eng.* **2011**, 46, 81-91.
29. Sivamani, S.; Prasad, B.S.; Nithya, K.; Sivarajasekar, N.; Hosseini-Bandegharaei, A. Back-propagation neural network: Box–Behnken design modelling for optimization of copper adsorption on orange zest biochar. *Int. J. Environ. Sci. Technol.* **2022**, 19, 4321-4336.
30. Sivamani, S.; Nazar, A. New Covid Cases in India during Second Wave: Data Prediction using Probability Modelling. *Int. J. Adv. Res. Eng. Manage.* **2021**, 7(8), 1-8.